Unique Distribution of Aromatase in the Human Brain: In Vivo Studies With PET and [*N*-Methyl-^{11}C]Vorozole

ANAT BIEGON,[1]* SUNG WON KIM,[2] DAVID L. ALEXOFF,[1] MILLARD JAYNE,[1] PAULINE CARTER,[1] BARBARA HUBBARD,[1] PAYTON KING,[1] JEAN LOGAN,[1] LISA MUENCH,[2] DEBORAH PARETO,[3] DAVID SCHLYER,[1] COLLEEN SHEA,[1] FRANK TELANG,[1] GENE-JACK WANG,[1,4] YOUWEN XU,[1] AND JOANNA S. FOWLER[1,4,5]

[1]*Medical Department, Brookhaven National Laboratory, Upton, New York*
[2]*National Institute on Alcoholism and Alcohol Abuse, Bethesda, Maryland*
[3]*Institut Alta Tecnologia, CIBER BBN, Barcelona, Spain*
[4]*Department of Psychiatry, Mount Sinai School of Medicine, New York, New York*
[5]*Department of Chemistry, State University of New York at Stony Brook, Stony Brook, New York*

KEY WORDS estrogen; testosterone; androgens; steroidogenesis; imaging

ABSTRACT Aromatase catalyzes the last step in estrogen biosynthesis. Brain aromatase is involved in diverse neurophysiological and behavioral functions including sexual behavior, aggression, cognition, and neuroprotection. Using positron emission tomography (PET) with the radiolabeled aromatase inhibitor [*N*-methyl-^{11}C]vorozole, we characterized the tracer distribution and kinetics in the living human brain. Six young, healthy subjects, three men and three women, were administered the radiotracer alone on two separate occasions. Women were scanned in distinct phases of the menstrual cycle. Specificity was confirmed by pretreatment with a pharmacological (2.5 mg) dose of the aromatase inhibitor letrozole. PET data were acquired over a 90-min period and regions of interest placed over selected brain regions. Brain and plasma time activity curves, corrected for metabolites, were used to derive kinetic parameters. Distribution volume (V_T) values in both men and women followed the following rank order: thalamus > amygdala = preoptic area > medulla (inferior olive) > accumbens, pons, occipital and temporal cortex, putamen, cerebellum, and white matter. Pretreatment with letrozole reduced V_T in all regions, though the size of the reduction was region-dependent, ranging from ~70% blocking in thalamus and preoptic area to ~10% in cerebellum. The high levels of aromatase in thalamus and medulla (inferior olive) appear to be unique to humans. These studies set the stage for the noninvasive assessment of aromatase involvement in various physiological and pathological processes affecting the human brain. **Synapse 64:801–807, 2010.**

INTRODUCTION

Aromatase, a member of the cytochrome P450 (CYP450) protein superfamily (Danielson, 2002), is a unique gene product of the CYP19 gene. Aromatase regulates the last step of estrogen biosynthesis, aromatizing the A ring of androgens such as androstenedione and testosterone to estrone and estradiol, respectively. Aromatase is expressed in various organs including the brain (Roselli, 2007; Simpson et al., 2002). Low levels of aromatase were found throughout the rat and monkey brain, with high levels present only in the preoptic area, ventromedial nucleus of the hypothalamus, medial amygdala, and the bed nucleus of the stria terminalis (Roselli et al., 2001; Takahashi et al., 2006). As for the human brain, aromatase enzymatic activity, immunoreactivity, and gene expression (mRNA) were reported in studies of specific brain regions, including the temporal cortex (Steckelbroeck et al., 1999), hypothalamic

Contract grant sponsor: US Department of Energy OBER; Contract grant number: DE-AC02-98CH10886; Contract grant sponsor: NIH; Contract grant numbers: R01 NS050285 (to AB), K05DA020001 (to JSF); Contract grant sponsor: General Clinical Research Center of Stony Brook University (NIH); Contract grant number: MO1RR10710.

*Correspondence to: Anat Biegon, PhD, Medical Department, Brookhaven National Laboratory, Upton, New York 11973, USA. E-mail: biegon@bnl.gov

Received 13 October 2009; Accepted 11 November 2009

DOI 10.1002/syn.20791

Published online 29 March 2010 in Wiley Online Library (wileyonlinelibrary.com).

and ventral forebrain nuclei (Ishunina et al., 2005), hippocampus (Stoffel-Wagner et al., 1999), and thalamus (Sasano et al., 1998). To date, there have been no published studies of aromatase distribution or regulation throughout the human brain, while animal studies suggest that brain aromatase activity is higher in adult males than in adult females and is modulated by changes in testosterone levels but not the phase of the female estrus cycle (Abdelgadir et al., 1994; Roselli et al., 1984; Rosselli and Resko, 2001).

Aromatase, along with specific estrogen receptors, has been implicated in cellular proliferation, reproduction, sexual behavior, aggression, cognition, memory, and neuroprotection in various animal species (Garcia-Segura, 2008; Roselli, 2007; Saldahana et al., 2009). Changes in aromatase activity are also implicated in a wide range of human diseases, including Alzheimer's disease (AD; Hiltunen et al., 2006), brain injury (Roselli, 2007), breast cancer (Bulun and Simpson, 2008), endometriosis (Fedele et al., 2008), and hepatic cancer (Miceli et al., 2009).

Aromatase inhibitors (AI) are a relatively new class of drugs that are gaining ground in the treatment of breast cancer (Budzar and Howell, 2001). AI are also used by body builders who self-administer these drugs to avoid feminizing effects of excess testosterone, the precursor to estrogen (Hartgens and Kuipers, 2004). The AI fall under two categories: (1) steroidal AI such as formestane and exemestane, which bind irreversibly to the active site in aromatase, and (2) nonsteroidal AI such as aminoglutethimide, fadrozole, anastrozole, letrozole, and vorozole, which bind competitively and reversibly (Budzar and Howell, 2001). Among the AI, vorozole ((*S*)-6-[(4-chlorophenyl)(1*H*-1,2,4-triazol-1-yl)methyl]-1-methyl-1*H*-benzotriazole), K_i = 0.7 nM (Vanden Bossche et al., 1990), and letrozole (Cohen et al., 2002; Iveson et al., 1993) have been labeled with carbon-11 using [^{11}C]methyl iodide and evaluated as radiotracers for in vivo imaging of brain aromatase in primates (Kil et al., 2009; Kim et al., 2009; Lidstrom et al., 1998; Takahashi et al., 2006). While [^{11}C]letrozole failed to show specific displaceable binding in vivo (Kil et al., 2009), [^{11}C]vorozole brain scans revealed high specific binding in the rhesus amygdala, similar to results obtained with autoradiography of the rat brain (Takahashi et al., 2006). We have recently reinvestigated and modified the radiosynthesis and purification of [^{11}C]vorozole (Kim et al., 2009). We found that the previously published method resulted in three labeled compounds, not two as originally reported. [^{11}C]vorozole and another labeled isomer were not separated in the prior work, and thus we developed an improved purification method that yielded pure [^{11}C]vorozole (Kim et al., 2009). The pure labeled vorozole was tested and validated in female baboons, with the highest binding occurring in the amygdala and hypothalamic/preoptic area (Kim et al., 2009).

Despite the importance of aromatase in physiological and pathological processes and the increasing use of AI, there are no published quantitative, noninvasive studies of the distribution and regulation of aromatase in living humans. We hereby show that [^{11}C]vorozole is a useful ligand for studies of aromatase in the human brain with a unique pattern of regional distribution.

METHODS

Subjects

Six young, healthy nonsmoking subjects, three men and three women, were included in the study, which was approved by the Institutional Review Board and the Radioactive Drug Research Committee of Stony Brook University/Brookhaven National Laboratory. All subjects gave written informed consent. The study inclusion criteria were age 21–40, good health, and ability to give informed consent. Subjects were excluded for recent or current use of steroids (including contraceptives), recreational drugs and medications affecting brain function, neurological/psychiatric/metabolic disorders, and pregnancy in females.

Study design

During the screening visit, women were asked to report the date of their last menstrual period and their PET studies were scheduled to coincide with the nearest midcycle, when plasma estrogen levels are at their highest, or during the menstrual/early follicular phase, when estrogen levels are lower. Men were scanned at baseline, ~2 weeks later (retest) and again (blocking study) 2 h after ingesting an oral dose (2.5 mg) of letrozole (Femara, e.g., Cohen et al., 2002). Blood samples were withdrawn from all subjects on the day of the PET study and gonadal hormone levels measured in the plasma in a commercial laboratory (Quest).

Radiotracer synthesis

Pure [^{11}C]vorozole was synthesized and purified as recently described (Kim et al., 2009). Briefly, to (*S*)-norvorozole (1 mg) in DMSO (300 μl) was added KOH (5 M, 1 μl). After vortexing for 30 s, the reaction mixture was transferred into a V-shape reaction vessel. [^{11}C]methyl iodide was purged into this solution at room temperature and peak trapping was observed by a pin-diode detector. After the vessel was heated to 90°C for 3 min, the reaction mixture was cooled and diluted with high-performance liquid chromatography (HPLC) eluent. The crude product in DMSO was chromatographed using a solvent mixture of water (pH = 3.0, adjusted with formic acid)/methanol

(45/55) at a flow rate 1 ml/min on a Luna PFP(2) (Phenomenex, 250 mm × 10 mm, 5 μm). [*N*-methyl-^{11}C] vorozole eluted at 24.5 min was collected. The HPLC solvent was removed by azeotropic evaporation with acetonitrile using a rotary evaporator under reduced pressure. The residue was taken up by saline (4 ml) and filtered through a 0.22 μm Millipore® filter (Millipore, Billerica, MA) into a sterile vial. The radiochemical purity for [^{11}C]vorozole was >99%, measured by analytical HPLC using aqueous formic acid solution (pH = 3.0)/methanol (1/2) at a flow rate of 1 ml/min on a Luna PFP(2) (250 mm × 4.6 mm, 5 μm; Phenomenex, Torrance, CA). Specific activity was calculated from the radioactivity and mass detected (UV-254 nm) during preparative HPLC and reported as the ratio of radioactivity/mass (Ci/μmol).

PET scans

PET images were acquired over a 90-min period using a whole body, high-resolution positron emission tomograph (Siemen's HR+, 4.5 × 4.5 × 4.8 mm, mo^3 at the center of field of view) in 3D dynamic acquisition mode as previously described (Kim et al., 2009). For each of the PET scans, subjects received an injection of [^{11}C]vorozole (3–8 mCi; specific activity >0.1 mCi/nmol at the time of injection). An arterial plasma input function for [^{11}C]vorozole was obtained from arterial blood samples withdrawn every 2.5 s for the first 2 min (Ole Dich automatic blood sampler), then at 3, 4, 5, 6, 8, 10, 15, 20, 30, 45, 60, and up to 90 min (end of study). All samples were centrifuged to obtain plasma which was counted, and selected samples were assayed for the presence of unchanged [^{11}C]vorozole.

Assay of unchanged [^{11}C]vorozole in plasma

The fraction of [^{11}C]vorozole remaining in plasma was determined by automated solid phase extraction (Alexoff et al., 1995) after validating by HPLC using conditions described previously (Kim et al. 2009). The automated assay consisted of the following steps. Plasma (0.4 ml) was added to 3 ml phosphate buffer (pH 7) and applied to a previously conditioned C18 cartridge (Varian BondElut LRC 500 mg, Varian, Walnut Creek, CA), which was then washed sequentially with 3× 5 ml of water. All wash fractions and the C18 cartridge were counted. The ratio of the radioactivity remaining on the C18 cartridge to that of the total radioactivity recovered is the percent unchanged tracer, after corrections for radioactive decay, background, and geometry-dependent counting efficiency (Alexoff et al., 1995). Radioactivity recovery was 90–110%.

Image analysis

Time frames were summed over the 90-min scanning period. The summed PET images were coregistered with structural 3D MR image of the same subject using PMOD software (PMOD Technologies, Zurich, Switzerland) when available to confirm the anatomical location of tracer accumulation. Regions of interest (ROIs), including amygdala, cerebellum, cortex, medulla, preoptic area, putamen, thalamus, and cortical white matter, were placed on the summed image and then projected onto the dynamic images to obtain time activity curves. Regions occurring bilaterally were averaged. C-11 concentration in each ROI was divided by the injected dose to obtain the % dose/cm^3.

Kinetic analysis

A two-compartment model (Gunn et al., 2001) was used to estimate the total tissue distribution volume, V_T, which includes free and nonspecifically bound tracer as well as specifically bound tracer (Innis et al., 2007). In terms of a two compartment model $V_T = k_1/k_2(1 + k_3/k_4)$. The four model parameters of the two-compartment model were optimized to obtain the best fit to the ROI data using routines from Numerical Recipes (Press et al., 1990).

RESULTS

Plasma levels of [*N*-methyl-^{11}C]vorozole rose very quickly (less than 1 min to peak), followed by a monophasic decrease. Tracer metabolism in plasma was slow, with ~80% of the radioactivity due to unchanged vorozole after 30 min and ~60% after 90 min with no apparent effect of sex or letrozole pretreatment (Fig. 1). The tracer showed fast brain

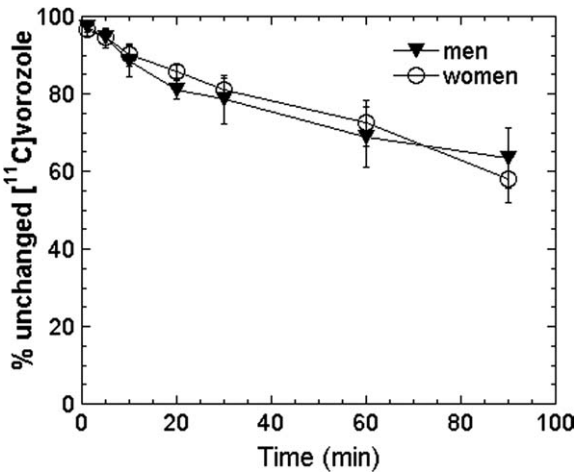

Fig. 1. Metablic stability of [^{11}C]vorozole in human plasma. Analysis was performed on plasma samples from three men and three women injected IV with [^{11}C]vorozole. The graph depicts means (SD) of % radioactivity identified as [^{11}C]vorozole at the specified time points.

penetration reaching peak values within less than 2 min, followed by a fast clearance stage and selective retention in specific regions such as thalamus and amygdala, where levels of radioactivity (decay corrected) were stable or even increased during the last 30 min of PET data acquisition (Fig. 2). This region-specific retention was completely blocked by pretreatment with letrozole (Fig. 2). Tracer distribution in the late (50–90 min post-tracer injection) time-frames was highly heterogeneous, with the highest levels seen in thalamus. Thalamic distribution was heterogeneous as well, with the highest levels in the paraventricular, dorsomedial, and pulvinar nuclei and lower binding in lateral and ventral thalamic nuclei (Figs. 2 and 3). Moderate levels of radioactivity were noted in amygdala and preoptic area/anterior hypothalamus and in the medulla (inferior olive). Cortical and basal ganglia levels were relatively low, with hippocampus indistinguishable from the temporal cortex. Accumbens levels in the basal ganglia were higher than those in caudate and putamen (Fig. 3).

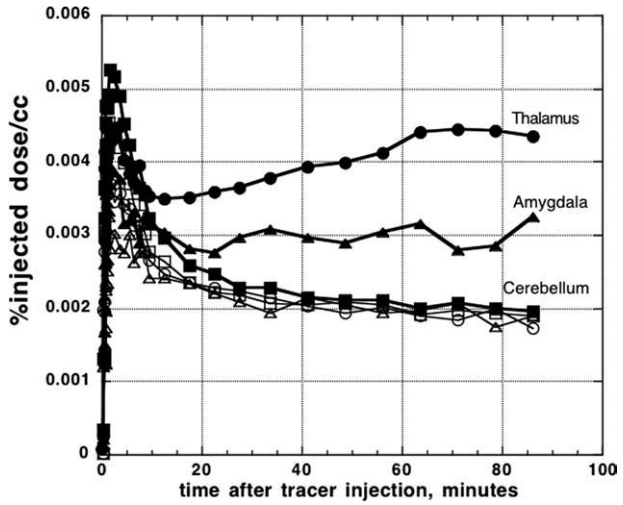

Fig. 2. Time-activity curves of [^{11}C]vorozole in human brain regions. Representative time activity curves in thalamus, amygdala, and cerebellum from one subject. Filled symbols depict a baseline (radiotracer only) scan and empty symbols depict a blocking study, with tracer injected 2 h after oral administration of letrozole (2.5 mg).

The regional distribution pattern illustrated in Figure 3 was observed in all of the subjects and scans in which the tracer was injected alone. The distribution volume (V_T) values derived from a two-compartment model in both men and women (regardless of menstrual cycle) followed the following rank order: thalamus > amygdala = preoptic area > medulla (inferior olive) cortex, putamen, cerebellum, and white matter (Figs. 4 and 5). Baseline and retest studies demonstrated the same regional rank order of tracer accumulation, with a trend toward lower V_T values in retest studies compared to baseline (Fig. 4).

Individual plasma testosterone and estrogen levels were within the established normal range for young men and women, with testosterone levels ranging from 250 to 570 ng/ml in men and <20–32 ng/ml in women and estrogen levels ranging from <50 to 114 pg/ml in men and 84–250 pg/ml in women.

Pretreatment with letrozole reduced V_T in all of the regions examined, resulting in a homogenous distribution across regions (Fig. 4). The size of the reduction was region-dependent, ranging from ~70% blocking in thalamus and preoptic area to ~10% in cerebellum (Fig. 4).

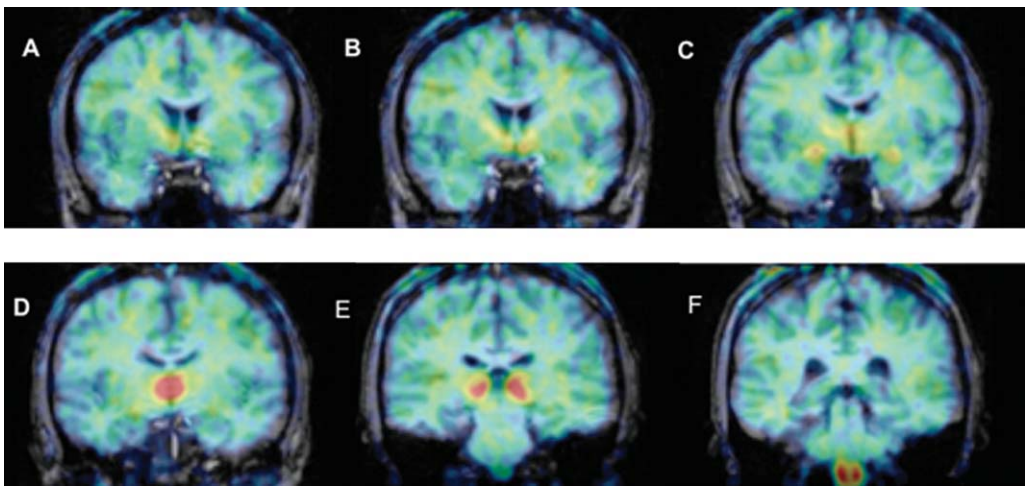

Fig. 3. Anatomical distribution of [^{11}C]vorozole in human brain. Figure shows coronal PET images (summed frames over 60–90 min, pseudocolored using the rainbow spectrum) overlaid on structural MRI (gray levels) of same subject. A = level of nucleus accumbens, B = level of anterior hypothalamus/preoptic area, C = level of amygdala, D = level of dorsomedial thalamus, E = level of pulvinar nucleus of thalamus, F = level of medulla/inferior olive. Note some radioactivity in cortical white matter but not in corpus callosum and relatively low levels in caudate and putamen (Levels A–C) and hippocampus (Levels D and E).

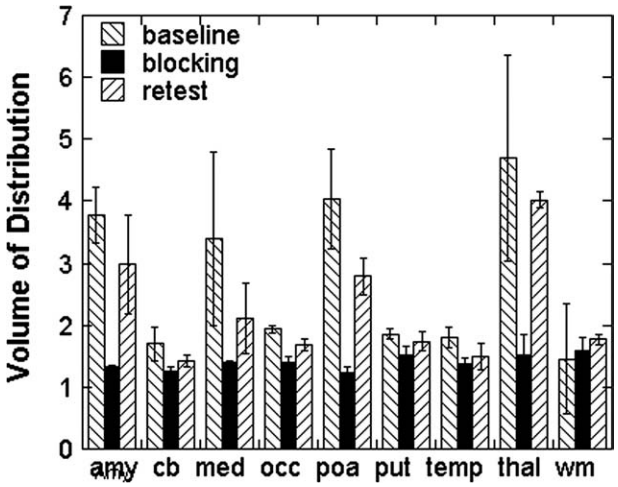

Fig. 4. Regional volume of distribution, reproducibility, and saturability of [^{11}C]vorozole in the brains of young men. Bars depict mean (SEM) of V_T following the first injection of tracer (baseline), tracer injection 2 h after letrozole (blocking), or tracer alone ~2 weeks after the first scan (retest). Amy, amygdala; cb, cerebellum; med, medulla (inferior olive); occ, occipital cortex; poa, preoptic area; put, putamen; temp, temporal cortex; thal, thalamus (pulvinar and mediodorsal); wm, cortical white matter.

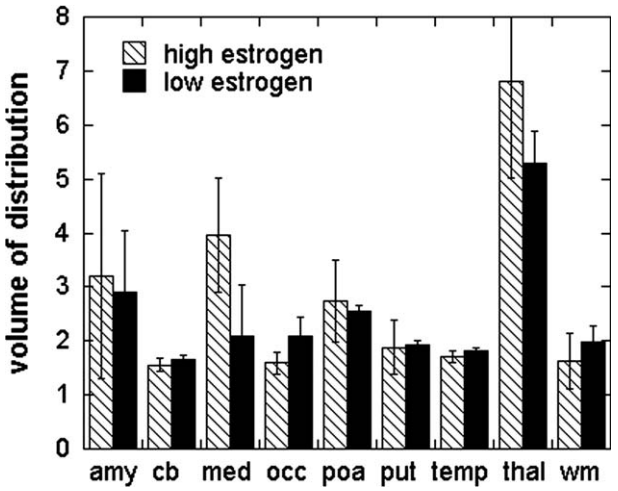

Fig. 5. Regional volume of distribution of [^{11}C]vorozole in the brains of young women. Bars depict mean (SEM) of V_T following injection of tracer in three women who were scanned around midcycle (12–17 days after onset of menses, when estrogen levels are at their highest, hatched bars) or during the menstrual/early follicular phase (27–4 days after onset of menses, when estrogen levels are low, black bars). Amy, amygdala; cb, cerebellum; med, medulla (inferior olive); occ, occipital cortex; poa, preoptic area; put, putamen; temp, temporal cortex; thal, thalamus (pulvinar and mediodorsal); wm, cortical white matter.

DISCUSSION

The results of the studies reported here suggest that [*N*-methyl-^{11}C]vorozole is a useful radiotracer for the noninvasive measurement of brain aromatase in humans, demonstrating anatomical and pharmacological specificity. Thus, the regional distribution pattern of the tracer was highly heterogeneous, with the highest levels found in distinct (dorsomedial, pulvinar, and paraventricular) thalamic nuclei, followed by moderately high levels in amygdala, preoptic area, and medulla and low levels in cortex, putamen, cerebellum, and cortical white matter. Tracer accumulation in all regions was reduced by oral pretreatment with the aromatase inhibitor letrozole (2.5 mg) given 2 h before tracer injection. This is in line with published studies performed in healthy volunteers, where the same dose of letrozole resulted in a near-complete inhibition of aromatase, expressed by a >80% decrease in plasma estrogen levels (Iveson et al., 1993). The time interval between pretreatment and tracer injection was also based on previous studies of peripheral inhibition of aromatase, where the effect of the drug peaked within 2–4 h of administration and lasted for more than 24 h (Iveson et al., 1993).

Previous PET studies with [^{11}C]vorozole (Lidstrom et al., 1998; Takahashi et al., 2006) did not report kinetic modeling of the tracer uptake but rather relied on region to cerebellum ratios at late time points. This approach, as well as a tissue reference model, was deemed inappropriate, since all gray matter regions, including the cerebellum, appeared to contain displaceable [^{11}C]vorozole binding in our baboon studies (Biegon et al., 2010; Kim et al., 2009) as well as in the present studies of the human brain. A comparison of one- and two-compartment models to the model-independent graphical approach (Logan et al., 2003) demonstrated a better fit of the two-compartment model, since the one-compartment model consistently underestimated the volume of distribution derived from the graphical analysis in baboons (Biegon et al., 2010). Therefore, we have used the two-compartment model to estimate the regional distribution volumes of [^{11}C]vorozole in the human brain. The regional rank order of V_T was similar to the %ID/CC observed at late (>50 min) but not early times after tracer injection.

The regional distribution pattern of aromatase in the human brain is strikingly different from the distribution reported in rodents and primates (baboon and rhesus), in which the highest levels were found in the amygdala and preoptic area while the levels in thalamus and medulla were unremarkable (Kim et al., 2009; Lidstrom et al., 1998; Takahashi et al., 2006). While difference between rodents and primates in brain receptor and enzyme distribution are common, primate and human brain usually show similar regional distribution patterns (e.g., Osterlund et al., 2001) making this an unexpected finding and suggesting a unique role for thalamic and medullar aromatase in humans.

Previous studies of human brain aromatase were conducted postmortem or on biopsy material and were confined to preselected, specific regions, such as

the temporal cortex (Stoffler-Wagner et al., 1999) or specific hypothalamic and ventral forebrain nuclei (Ishunina et al., 2005). Our results are in line with Sasano et al. (1998) who measured aromatase gene expression in thalamus as well as eight other regions and found high levels of aromatase gene expression in thalamus, while confirming the presence of aromatase in all other regions investigated. Although the number of subjects in our study is too small for formal statistical analysis, we did not find higher levels in men compared to women, as expected from the findings of Sasano et al. (1998), Steckelbroeck et al. (1999), Stoffel-Wagner et al. (1999), and Ishunina et al. (2005), who reported similar levels of brain aromatase activity and gene expression in men and women. Conversely, results from animal studies demonstrated higher levels of brain aromatase in males and suggested testosterone was a positive modulator of aromatase in the hypothalamic–preoptic area (Abdelgadir et al., 1994; Roselli et al., 1984). However, brain aromatase did not appear to be significantly regulated by the estrous cycle in rodents (Roselli et al., 1984), matching our results in a small number of women imaged at opposite phases of the menstrual cycle. Taken together, our findings support the notion that brain aromatase expression is regulated in a species- and region-selective manner (Roselli et al., 1984). Such specific regulation may be the result of tissue-specific aromatase promoters, which were identified in animal and human tissues (Golovine et al., 2003; Jones et al., 2006). Since other promoters besides the brain specific exon 1.f (Sasano et al., 1998) are expressed in the human brain, this heterogeneity may provide the basis for brain region-specific regulation and expression of aromatase in humans.

At present, we do not know which brain functions are served by the estrogen produced locally in the thalamus and inferior olive or the identity of the relevant estrogen receptor subtypes. Although the exact functions subserved by the human inferior olive are not clear, available information implicates this nucleus as well as specific thalamic nuclei in cognitive aspects of sensory and motor information processing, which may be modulated by estrogen (Liu et al., 2008; Ward et al., 2007).

As for the estrogen receptors, both ERα and ERβ receptors are expressed in a subtype-specific manner in the human brain, with ERα mostly restricted to hypothalamus and amygdala while ERβ expression is more widespread and found also in hippocampus, cortex, and thalamus (Osterlund et al., 2000). It is also possible that estrogen synthesized in thalamus and medulla interacts with the more recently characterized membranal estrogen receptors (Qiu et al., 2008; Toran-Allerand, 2004), some of which are expressed in regions lacking classical ERα and ERβ such as striatum and medulla in rats (Brailoiu et al., 2007). However, the regional distribution of membranal estrogen receptors in the human brain has not been reported to date.

In summary, [*N*-methyl-^{11}C]vorozole is a useful tracer for aromatase in the human brain, showing fast brain penetration and a unique pattern of binding in specific brain regions. These studies set the stage for the noninvasive assessment of aromatase involvement in various physiological, pathological, and pharmacological processes affecting the human brain.

ACKNOWLEDGMENTS

We thank Michael Schueller for cyclotron operations, Donald Warner for PET operations, and Karen Apelskog-Torres for study protocol preparation. We are also grateful to the people who volunteered for this study.

REFERENCES

Abdelgadir SE, Resko JA, Ojeda SR, Lephart ED, McPhaul MJ, Roselli CE. 1994. Androgens regulate aromatase cytochrome P450 messenger ribonucleic acid in rat brain. Endocrinology 135:395–401.

Alexoff DL, Shea C, Wolf AP, Fowler JS, King P, Gatley SJ, Schlyer DJ. 1995. Plasma input function determination for PET using a commercial laboratory robot. Nucl Med Biol 22:893–904.

Biegon A, Kim, S-W, Logan J, Hooker JM, Muench L, Fowler JS. 2010. Nicotine blocks brain estrogen synthase (aromatase): In vivo PET studies in female baboons. Biol Psychiatry. Feb 24 Epub ahead of print.

Brailoiu E, Dun SL, Brailoiu GC, Mizuo K, Sklar LA, Oprea TI, Prossnitz ER, Dun NJ. 2007. Distribution and characterization of estrogen receptor G protein-coupled receptor 30 in the rat central nervous system. J Endocrinol 193:311–321.

Budzar A, Howell A. 2001. Advances in aromatase inhibition: Clinical efficacy and tolerability in the treatment of breast cancer. Clin Cancer Res 7:2620–2635.

Bulun SE, Simpson ER. 2008. Aromatase expression in women's cancers. Adv Exp Med Biol 630:112–132.

Cohen MH, Johnson JR, Li N, Chen G, Pazdur R. 2002. Approval summary: Letrozole in the treatment of postmenopausal women with advanced breast cancer. Clin Cancer Res 8:665–669.

Danielson PB. 2002. The cytochrome P450 superfamily: Biochemistry, evolution and drug metabolism in humans. Curr Drug Metab 3:561–597.

Fedele L, Somigliana E, Frontino G, Benaglia L, Vigano P. 2008. New drugs in development for the treatment of endometriosis. Expert Opin Investig Drugs 17:1187–1202.

Garcia-Segura LM. 2008. Aromatase in the brain: Not just for reproduction anymore J Neuroendocrinol 20:705–712.

Golovine K, Schwerin M, Vanselow J. 2003. Three different promoters control expression of the aromatase cytochrome p450 gene (cyp19) in mouse gonads and brain. Biol Reprod 68:978–984.

Gunn RN, Gunn SR, Cunningham VJ. 2001. Positron emission tomography compartmental models. J Cereb Blood Flow Metab 21: 635–652.

Hartgens F, Kuipers H. 2004. Effects of androgenic–anabolic steroids in athletes. Sports Med 34:513–554.

Hiltunen M, Iivonen S, Soininen H. 2006. Aromatase enzyme and Alzheimer's disease. Minerva Endocrinol 31:61–73.

Innis RB, Cunningham VJ, Delforge J, Fujita M, Giedde A, Gunn RN, Holden J, Houle S, Huang SC, Ichise M, Lida H, Ito H, Kimura Y, Koeppe RA, Knudsen GM, Knuuti J, Lammertsma AA, Laruelle M, Logan J, Maguire RP, Mintun MA, Morris ED, Parsey R, Price JC, Slifstein M, Sossi V, Suhara T, Votaw JR, Wong DF, Carson RE. 2007. Consensus nomenclature for in vivo imaging of reversibly binding radioligands. J Cereb Blood Flow Metab 27: 1533–1539.

Ishunina TA, van Beurden D, van der Meulen G, Unmehopa UA, Hol EM, Huitinga I, Swaab DF. 2005. Diminished aromatase immunoreactivity in the hypothalamus, but not in the basal forebrain nuclei in Alzheimer's disease. Neurobiol Aging 26:173–194.

Iveson TJ, Smith IE, Ahern J, Smithers DA, Trunet PF, Dowsett M. 1993. Phase I study of the oral nonsteroidal aromatase inhibitor CGS 20267 in healthy postmenopausal women. J Clin Endocrinol Metab 77:324–331.

Jones ME, Boon WC, Proietto J, Simpson ER. 2006. Of mice and men: The evolving phenotype of aromatase deficiency. Trends Endocrinol Metab 17:55–64.

Kil KE, Biegon A, Ding YS, Fischer A, Ferrieri RA, Kim SW, Pareto D, Schueller MJ, Fowler JS. 2009. Synthesis and PET studies of [(11)C-cyano]letrozole (Femara), an aromatase inhibitor drug. Nucl Med Biol 36:215–223.

Kim SW, Biegon A, Katsamanis Z, Erlich CW, Hooker JM, Shea C, Muench L, Xu Y, King P, Alexoff D, Fowler JS. 2009. Reinvestigation of the synthesis and evaluation of [*N*-methyl-11C]vorozole, a radiotracer targeting cytochrome P450 aromatase. Nucl Med Biol 36:323–334.

Lidström P, Bonasera TA, Kirilovas D, Lindblom B, Lu L, Bergström E, Bergström M, Westlin J-E, Långström B. 1998. Synthesis, in vivo rhesus monkey biodistribution and in vitro evaluation of a 11C-labelled potent aromatase inhibitor: [*N*-methyl-11C]vorozole. Nucl Med Biol 25:497–501.

Liu T, Xu D, Ashe J, Bushara K. 2008. Specificity of inferior olive response to stimulus timing. J Neurophysiol 100:1557–1561.

Logan J. 2003. A review of graphical methods for tracer studies and strategies to reduce bias. Nucl Med Biol 30:833–844.

Miceli V, Cervello M, Azzolina A, Montalto G, Calabrò M, Carruba G. 2009. Aromatase and amphiregulin are correspondingly expressed in human liver cancer cells. Ann N Y Acad Sci 1155: 252–256.

Österlund MK, Gustafsson JA, Keller E, Hurd YL. 2000. Estrogen receptor beta (ERbeta) messenger ribonucleic acid (mRNA) expression within the human forebrain: Distinct distribution pattern to ERalpha mRNA. J Clin Endocrinol Metab 85:3840–3846.

Österlund MK, Yasmin L, Hurd YL. 2001. Estrogen receptors in the human forebrain and the relation to neuropsychiatric disorders. Prog Neurobiol 64:251–267.

Press W, Flannery B, Teukolsky S, Vetterline W. 1990. Numerical recipes in C: The art of scientific computing. Cambridge: Cambridge University Press.

Qiu J, Ronnekleiv OK, Kelly MJ. 2008. Modulation of hypothalamic neuronal activity through a novel G-protein-coupled estrogen membrane receptor. Steroids 73:985–991.

Roselli CE. 2007. Brain aromatase: Roles in reproduction and neuroprotection. J Steroid Biochem Mol Biol 106:143–150.

Roselli CE, Resko JA. 2001. Cytochrome P450 aromatase (CYP19) in the non-human primate brain: Distribution, regulation, and functional significance. J Steroid Biochem Mol Biol 79:247–253.

Roselli CE, Ellinwood WE, Resko JA. 1984. Regulation of brain aromatase activity in rats. Endocrinology 114:192–200.

Roselli CE, Klosterman S, Resko JA. 2001. Anatomic relationships between aromatase and androgen receptor mRNA expression in the hypothalamus and amygdala of adult male cynomolgus monkeys. J Comp Neurol 439:208–223.

Sasano H, Takahashi K, Satoh F, Nagura H, Harada N. 1998. Aromatase in the human central nervous system. Clin Endocrinol 48: 325–329.

Saldahana CJ, Duncan KA, Walters BJ. 2009. Neuroprotective actions of brain aromatase. Front Neuroendocrinol 30:106–118.

Simpson ER, Clyne C, Rubin G, Boon WC, Robertson K, Britt K, Speed C, Jones M. 2002. Aromatase—A brief overview. Annu Rev Physiol 64:93–127.

Steckelbroeck S, Heidrich DD, Stoffel-Wagner B, Hans VHJ, Schramm J, Bidlingmaier F, Klingmüller D. 1999. Characterization of aromatase cytochrome P450 activity in the human temporal lobe. J Clin Endocrinol Metab 84:2795–2801.

Stoffel-Wagner B, Watzka M, Schramm J, Bidlingmaier F Klingmüller D. 1999. Expression of CYP19 (aromatase) mRNA in different areas of the human brain. J Steroid Biochem Mol Biol 70:237–241.

Takahashi K, Bergström M, Frändberg P, Vesström E-L, Watanabe Y, Långström B. 2006. Imaging of aromatase distribution in rat and rhesus monkey brains with [11C]vorozole. Nucl Med Biol 33: 599–605.

Toran-Allerand CD. 2009. Minireview: A plethora of estrogen receptors in the brain: Where will it end? Endocrinology 145:1069–1074.

Vanden Bossche H, Willemsens G, Roels I, Bellens D, Moereels H, Coene M-C, Le Jeune L, Lauwers W, Janssen PAJ. 1990. R76713 and enantiomers: Selective nonsteroidal inhibitors of the cytochrome P450-dependent oestrogen synthesis. Biochem Pharmacol 40:1707–1718.

Ward R, Arend I. 2007. An object-based frame of reference within the human pulvinar. Brain 130:2462–2469.

Wu MV, Manoli DS, Fraser EJ, Coats JK, Tollkuhn J, Honda S, Harada N, Shah NM. 2009. Estrogen masculinizes neural pathways and sex-specific behaviors. Cell 139:61–72.